Turkish Journal of Earth Sciences (Turkish J. Earth Sci.), Vol. 21, 2012, pp. 19–35. Copyright ©TÜBİTAK
doi:10.3906/yer-1006-14 First published online 23 January 2011

The Kemer Metamorphic Complex (NW Turkey): A Subducted Continental Margin of the Sakarya Zone

MESUT AYGÜL[1], GÜLTEKİN TOPUZ[1], ARAL I. OKAY[1], MUHARREM SATIR[2] & HANS-PETER MEYER[3]

[1] İstanbul Teknik Üniversitesi, Avrasya Yerbilimleri Enstitüsü, TR–34469, Maslak, İstanbul, Turkey
(E-mail: aygulm@itu.edu.tr)
[2] Universität Tübingen, Institut für Geowissenschaften, Wilhelmstrasse 56, D-72074 Tübingen, Germany
[3] Universität Heidelberg, Institut für Geowissenschaften, Im Neuenheimer Feld 234-236,
D-69120 Heidelberg, Germany

Received 22 June 2010; revised typescript received 05 November 2011; accepted 23 January 2011

Abstract: High-pressure and ultrahigh-pressure metamorphic rocks crop out widely in the northern Aegean. In many instances their ages and tectonic setting are poorly constrained. Here we report newly discovered high-pressure rocks of continental crustal origin and of Late Cretaceous age southwest of the Marmara Sea. They occur at the contact between the Rhodope-Strandja Zone in the north and the Sakarya Zone in the south.

The Kemer Metamorphic Complex is composed mainly of mica schist, calcschist and marble with minor metabasite and serpentinite. The mica schists contain garnet, phengite (3.30-3.44 c.p.f.u), (±) paragonite, albite, epidote, calcite, chlorite and titanite. The high-pressure metamorphic origin of the mica schists is shown by the high silica contents of the white micas and by glaucophane inclusions in garnet. In the metabasites the mineral assemblage is garnet, barroisite, epidote, albite, titanite, quartz, phengite and chlorite; no evidence is left for the former presence of high-pressure minerals. Metamorphic conditions are constrained by mineral equilibria: a 560–640°C temperature at a minimum pressure of 10 kbar. The metamorphism is dated at 64–84 Ma by the Rb-Sr phengite-whole rock method.

The Kemer Metamorphic Complex is in tectonic contact with an accretionary ophiolitic mélange consisting of limestone, basalt, serpentinite, greywacke, radiolarian chert and metabasite. Some of the metabasites in the mélange contain Na-amphibole and lawsonite, indicating a subduction origin. The ages of the limestone blocks in the mélange range from Late Triassic to Late Cretaceous and that of the radiolarite blocks from Middle Jurassic to Early Cretaceous, indicating an oceanic domain dating back to Late Triassic at least. The Kemer Metamorphic Complex and the Çetmi Mélange are intruded by a granodiorite of Early Eocene (52 Ma) age and are unconformably covered by a Late Eocene volcano-sedimentary succession.

The lithology of the Kemer Metamorphic Complex resembles a continental margin rather than an oceanic accretionary complex. This and the presence of a Late Cretaceous magmatic arc in the north (Sredna-Gora-Pontide) suggest that the Kemer metamorphic rocks were initially deposited on the northern passive margin of the Sakarya Zone, which was subducted under the Rhodope-Strandja continental domain.

Key Words: Kemer Metamorphic Complex, ophiolitic mélange, HP/LT metamorphism, Sakarya Zone, continental margin

Sakarya Zonu'nun Yitime Uğramış Kıta Kenarı: Kemer Metamorfik Karmaşığı (KB Türkiye)

Özet: Yüksek-basınç ve aşırı yüksek-basınç metamorfik kayaları kuzey Ege'de geniş alanlarda yüzeylemektedir. Bir çok durumda, bu kayaçların yaşları ve tektoniği kısmen belirlenebilmiştir. Bu çalışmada Marmara Denizi'nin güneybatısında keşfedilen kıtasal kökenli Geç Kretase yaşlı yüksek-basınç metamorfik kayaları rapor edilmektedir. Bu metamorfik kayalar kuzeyde Rodop-Istranca Zonu ile güneydeki Sakarya Zonu arasında yer almaktadır.

Kemer Metamorfik Karmaşığı baskın olarak mikaşist, kalkşist ve mermerler ile tali oranda ki metabazit ve serpantinitlerden oluşmaktadır. Mikaşistler granat, fengit (3,30–3,44 c.p.f.u), (±) paragonit, albit, epidot, kalsit, klorit ve titanitten oluşmaktadır. Ak mikaların yüksek silika içerikleri ve granatlarda bulunan glokofan kapanımları mikaşistlerin yüksek-basınç başkalaşımına maruz kaldığını göstermektedir. Metabazitlerin mineral birlikteliği granat, barroyisit, epidot, albit, titanit, kuvars, fengit ve klorit olup, yüksek-basınç başkalaşımının izleri ortadan kalkmıştır. Başkalaşımın doruk koşulları denge mineral toplulukları kullanılarak minimum 10 kbar basınç için 560–640°C sıcaklık olarak sınırlandırılmıştır. Başkalaşımın yaşı Rb-Sr fengit-toplam kayaç yöntemiyle 64–84 Ma olarak saptanmıştır.

Kemer Metamorfik Karmaşığı, kireçtaşı, basalt, serpantinit, grovak, radyolaryalı çört ve metabazit blokları içeren bir ofiyolitik melanj ile tektonik dokanaklıdır. Bazı metabazitlerin Na-amfibol ve lavsonit içermeleri karmaşığın dalma-batma kökenli olduğunu işaret etmektedir. Melanj içerisindeki kireçtaşı bloklarının yaşları Geç Triyas–Geç Kretase, radyolaritlerin yaşları ise Orta Jura–Erken Kretase arasındadır. Kemer Metamorfik Karmaşığı ve Çetmi Melanjı Erken Eosen (52 Ma) yaşlı bir granitoyid tarafından kesilmekte ve Geç Eosen yaşlı volcano-sedimenter kayalar tarafından uyumsuzlukla örtülmektedir.

Kemer Metamorfik Karmaşığı'nın litolojisi okyanusal yığışım karmaşığından ziyade kıta kenarını işaret etmektedir. Bu durum ve kuzeyde mağmatik bir yayın (Sredna-Gora-Pontid) varlığı, Kemer Metamorfik Karmaşığı'nın ilksel olarak Sakarya Zonu'nun kuzey kenarında çökeldiğini ve Rodop-Istranca kıtasal alanının altına daldığını göstermektedir.

Anahtar Sözcükler: Kemer Metamorfik Karmaşığı, ofiyolitik melanj, YB/DS başkalaşımı, Sakarya Zonu, kıta kenarı

Introduction

The geology of Turkey is mainly controlled by the consumption of the Tethyan oceans during the evolution of the Alpine-Himalayan orogeny (Şengör & Yılmaz 1981; Okay & Tüysüz 1999). During the orogeny different continental fragments or terranes were juxtaposed along the suture zones, which are marked by oceanic accretionary complexes, ophiolites and high-pressure metamorphic rocks. The Biga Peninsula in NW Turkey is characterized by ophiolites, ophiolitic mélanges and high-pressure metamorphic rocks, which separate two different tectonic units: the Rhodope-Strandja Zone in the north and the Sakarya Zone in the south (Figure 1). The ophiolitic mélanges and ophiolites in this region have been interpreted as vestiges of the former Intra-Pontide Ocean (Şengör & Yılmaz 1981; Okay *et al.* 1991; Okay & Tansel 1994). However, the absence of quantitative geochronological and petrological data from the metamorphic rocks and ophiolitic mélange makes their tectonic significance ambiguous. Here we report new petrological and geochronological data from the Kemer region on the northern margin of the Biga Peninsula, where both ophiolitic mélange and high-pressure rocks are widely exposed. The data are discussed in terms of the geodynamic evolution of the Intra-Pontide Ocean.

Regional Tectonic Framework

The Rhodope-Strandja-Circum-Rhodope and the Sakarya zones, along with the İstanbul Zone, make up the Pontides, which are separated by the Neo-Tethyan İzmir-Ankara-Erzincan Suture from the Anatolide-Tauride Block of Gondwanaland origin (Şengör & Yılmaz 1981; Okay 1989; Okay & Tüysüz 1999). Ophiolitic mélanges crop out between the İstanbul and Sakarya zones, where they are interpreted as the remnants of the Intra-Pontide Ocean (Şengör & Yılmaz 1981). Below, we outline the main tectonostratigraphic features of the relevant units in the Rhodopes and the Pontides.

The Rhodope Massif and the Circum Rhodope Belt

The Rhodope Massif, widely exposed in northern Greece and Bulgaria, consists of high-grade metamorphic rocks of both continental and oceanic affinity. It is structurally divided into lower and upper units (Burg *et al.* 1996; Ricou *et al.* 1998). The lower unit consists of ortho- and paragneisses with eclogitic amphibolites. The upper unit includes gneiss, amphibolite, schist and marble, with metaperidotite and eclogite slices. In the lower unit, inclusions of microdiamond and quartz pseudomorphs after coesite in garnet are reported from some eclogites indicating ultrahigh-pressure conditions (Mposkos & Kostopoulos 2001).

The Rhodope Massif is tectonically overlain in the east by a low-grade metasedimentary and metavolcanic succession belonging to the Circum-Rhodope belt, which is interpreted as a marginal basin and volcanic arc suite deformed and metamorphosed during Late Jurassic–Early Cretaceous time (Magganas 2002; Bonev & Stampfli 2008). Okay *et al.* (2010) reported a possible eastern extension of the Circum-Rhodope into the Mecidiye region, southern Thrace. It comprises low-grade slate, phyllite and limestone, unconformably overlain by Upper Eocene clastics and limestone.

The Strandja Massif

The Strandja Massif is generally linked with the Rhodope and Serbo-Macedonian massifs. Its basement is composed of gneiss and amphibolites

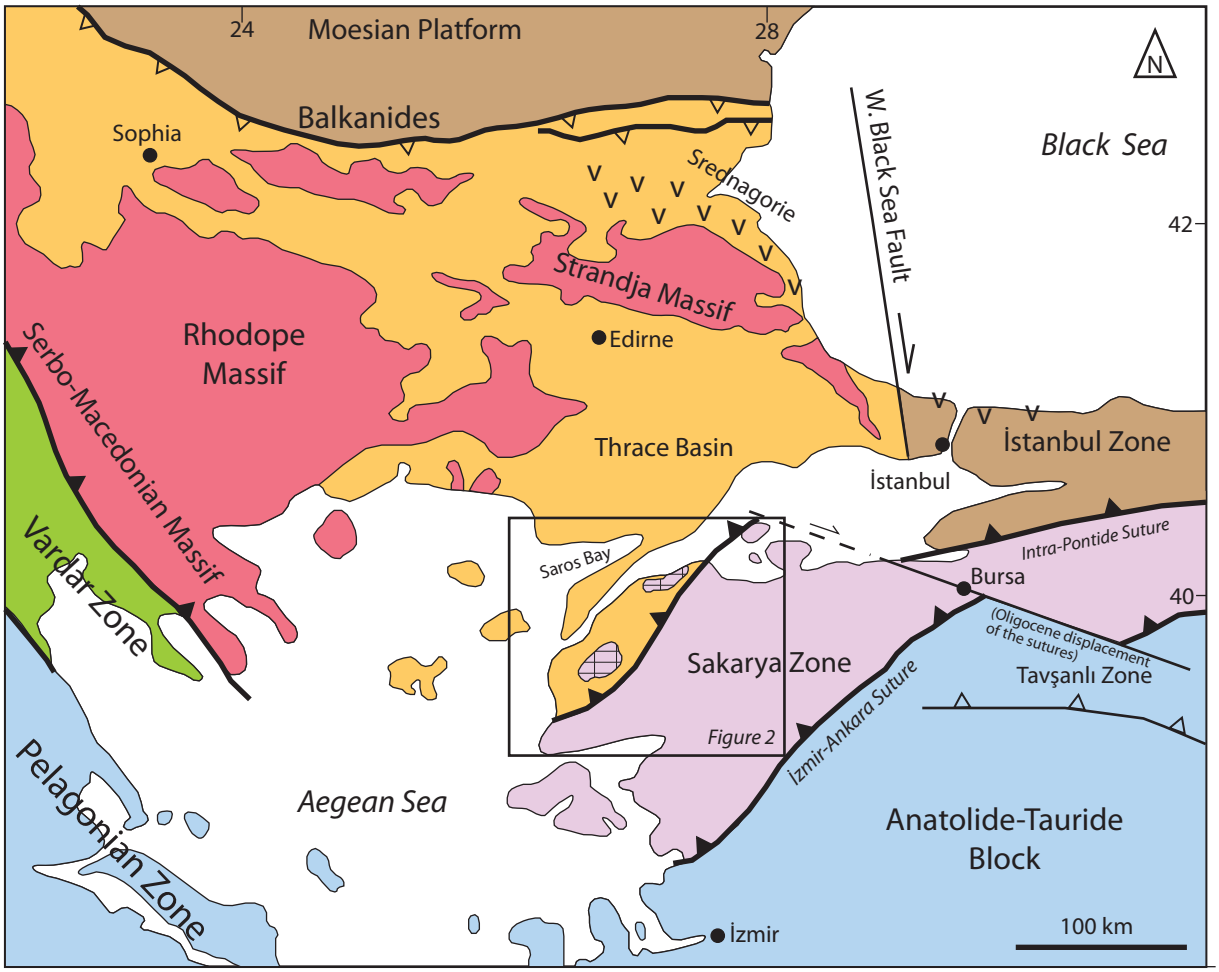

Figure 1. Tectonic map of the northern Aegean and surrounding areas showing the location of the Çamlıca and Kemer Metamorphic Complex (modified from Okay & Satır 2000a).

intruded by Late Carboniferous to Early Permian granites (Okay *et al.* 2001; Sunal *et al.* 2006, 2008, 2011). This basement is unconformably overlain by an Lower Triassic–Middle Jurassic epicontinental sequence. The basement rocks and sedimentary cover rocks were regionally deformed and metamorphosed during the Late Jurassic–Early Cretaceous. The metamorphism was associated with north-vergent thrusts. Finally, the metamorphic rocks were unconformably overlain by Upper Cretaceous (Cenomanian) sedimentary and volcanic rocks.

The Sakarya Zone

The Sakarya Zone has a high-grade metamorphic basement consisting of gneiss, amphibolite and marble exposed in the Kazdağ, Uludağ and Pulur regions. The age of high-grade metamorphism is Carboniferous (330–310 Ma) (Okay *et al.* 1996, 2006; Topuz *et al.* 2004a, 2008). The high-grade metamorphic rocks are intruded by Carboniferous granites (Topuz *et al.* 2010). A subduction-accretion complex, known as the Karakaya Complex, was accreted to the basement rocks during the latest Triassic (Okay & Monie 1997; Okay *et al.* 2002; Okay & Göncüoğlu 2004; Topuz *et al.* 2004b). The Karakaya Complex is unconformably overlain by a transgressive sequence, starting with Lower Jurassic shallow marine clastics followed by Upper Jurassic–Lower Cretaceous limestones.

Geological Setting

The Rhodope Massif in the Biga Peninsula is represented by metamorphic rocks, which crop out in two main areas (Okay & Satır 2000a, b; Beccaletto & Jenny 2004; Beccaletto *et al.* 2007) (Figure 2). In the south the Çamlıca Metamorphic Complex is dominated by quartz-feldspar-rich schists with minor calcschist, marble and metabasite. Virtually all metabasites contain only greenschist-facies mineral assemblages, except for a few eclogite and eclogitic amphibolite bands within the quartzo-feldspathic mica schists (Okay & Satır 2000a). The Çamlıca Metamorphic Complex is considered to have undergone a HP/LT metamorphism at a minimum pressure of 11 kbar and at a temperature of 510±50°C, followed by strong retrogression. Phengite Rb-Sr dates from the quartzo-feldspathic schists indicate a Late Cretaceous age (65–70 Ma) for the metamorphism. In the west the Çamlıca Metamorphic Complex is in steep tectonic contact with the Denizgören ophiolite, consisting mainly of peridotite. Ar-Ar hornblende ages from the metamorphic sole of this ophiolite are mid-Cretaceous (117 Ma, Okay *et al.* 1996; 125 Ma, Beccaletto & Jenny 2004) suggesting an Aptian emplacement for the ophiolite. In the west, the Denizgören ophiolite overlies a low-grade metamorphic sequence consisting of Permian recrystallized limestone and Triassic flysch (Okay *et al.* 1991; Beccaletto & Jenny 2004).

Metamorphic rocks, lithologically similar to the Çamlıca Metamorphic Complex but without eclogites, crop out in the northern part of the Biga Peninsula (Okay *et al.* 1991; Okay & Satır 2000a; Beccaletto *et al.* 2007; Figure 2). This Kemer Metamorphic Complex is in tectonic contact in the south with an ophiolitic mélange, which marks the tectonic boundary between the Sakarya and Rhodope zones in the Biga Peninsula. We studied the Kemer Metamorphic Complex and the adjacent mélange through detailed geological mapping, petrology and geochronology (Figure 3).

The Kemer Metamorphic Complex

The Kemer Metamorphic Complex is composed predominantly of mica schist, calcschist, marble and minor amounts of metabasite and serpentinite. Mica schists, which make up *ca.* 80% of the outcrop area, are generally grey to greyish green and show well-developed foliation and shear fabrics. They gradually pass into white calcschist and thickly banded marbles. Metabasites constitute a small part (<5%) of the metamorphic sequence. In the garnet-mica schists, they form laterally discontinuous lenses, 0.5–1.5 m thick. Serpentinites form well-foliated small (2–3 m in width) tectonic slivers in the mica schists with Mg-rich amphibole, epidote and talc along their contacts, possibly due to metasomatic growth.

Garnet-mica schists contain quartz, white mica, albite and minor amounts of garnet, epidote, calcite, chlorite and titanite. Garnets occur only in the northwestern part of the region (Figure 3). They show syntectonic rotational internal fabrics and have inclusions of epidote, quartz, phengite, titanite, rutile, chloritoid and glaucophane. Secondary muscovite and chlorite grew in cracks and at the edges of the garnet crystals. Five representative samples from the garnet mica schists were analyzed by electron microprobe. The analytical techniques are described in the Appendix. The estimated modes of these samples and representative mineral compositions are given in Tables 1 and 2, respectively.

Garnets have a compositional range of $Alm_{50-74}Grs_{24-32}Sps_{11-03}Pyp_{03-23}$. They typically show prograde zonation with an increase in the almandine and pyrope components and a decrease in the spessartine component from core to rim (Figure 4a, b). Ferroglaucophane occurs as inclusions in garnet in one of the mica schist samples. Garnet from another sample has chloritoid inclusions with Fe/(Fe+Mg) ratios between 0.86–0.90. Primary white micas are phengitic, with Si contents ranging between 3.30–3.44 cpfu (Figure 5). Secondary muscovite occurs in samples 218 and 219, with Si-values decreasing to 3.1. Plagioclase is nearly pure albite. Epidotes are generally rich in allanite component in the core but some epidotes also have allanite rims. The $Fe^{3+}/(Fe^{3+}+Al)$ ratios of the epidotes range between 0.13 and 0.18 and generally increases rimward. One sample (K3/5) also contains paragonite in the matrix. Titanite is a stable phase in the matrix and replaces rutile. Ilmenite is observed as a matrix phase in the samples 218 and 219, and as inclusions in garnet in sample K3/5.

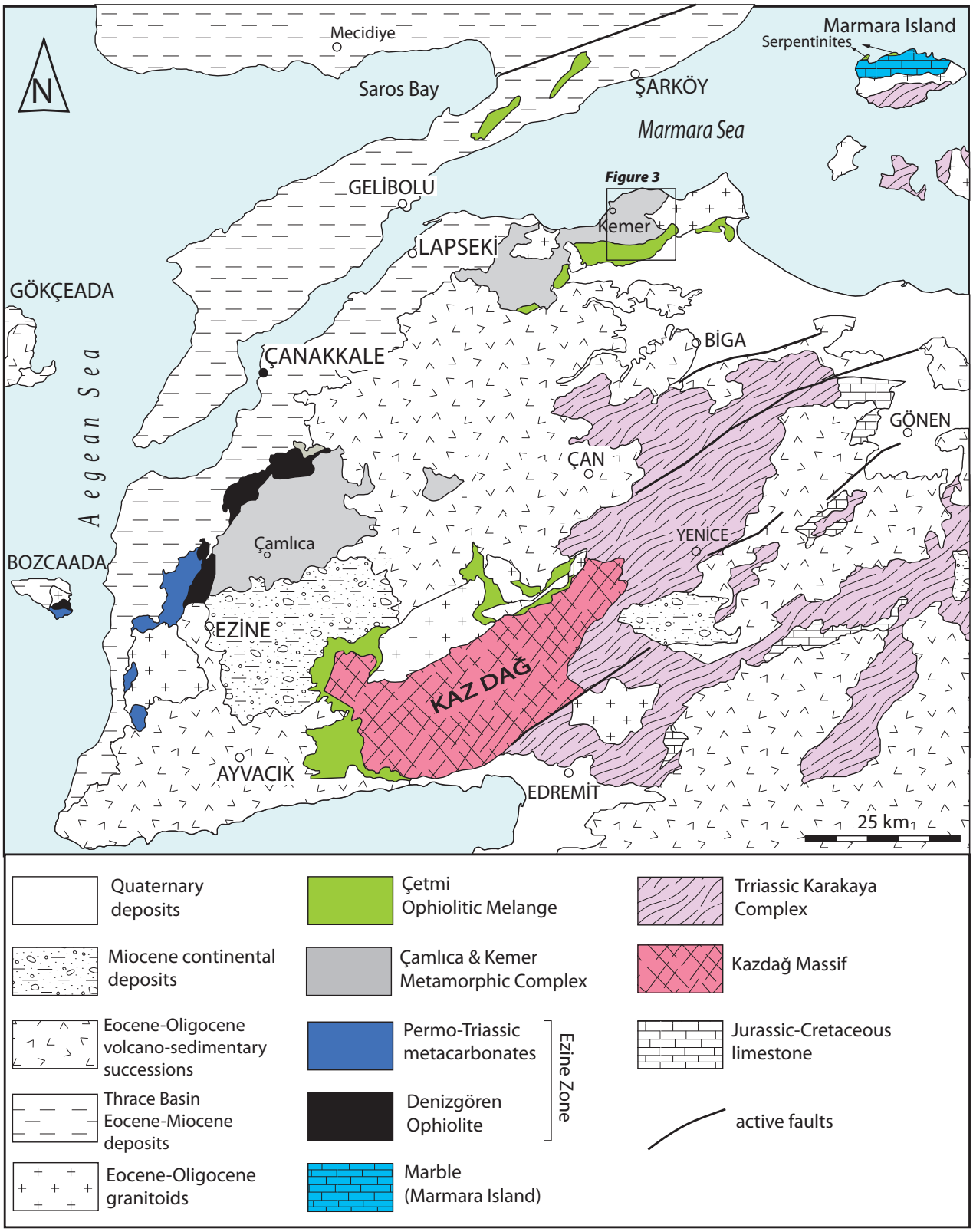

Figure 2. Geological maps of the Biga and Gelibolu peninsulas (modified from Okay *et al.* 1991; Okay & Satır 2000a; Türkecan & Yurtsever 2002; Konak 2002).

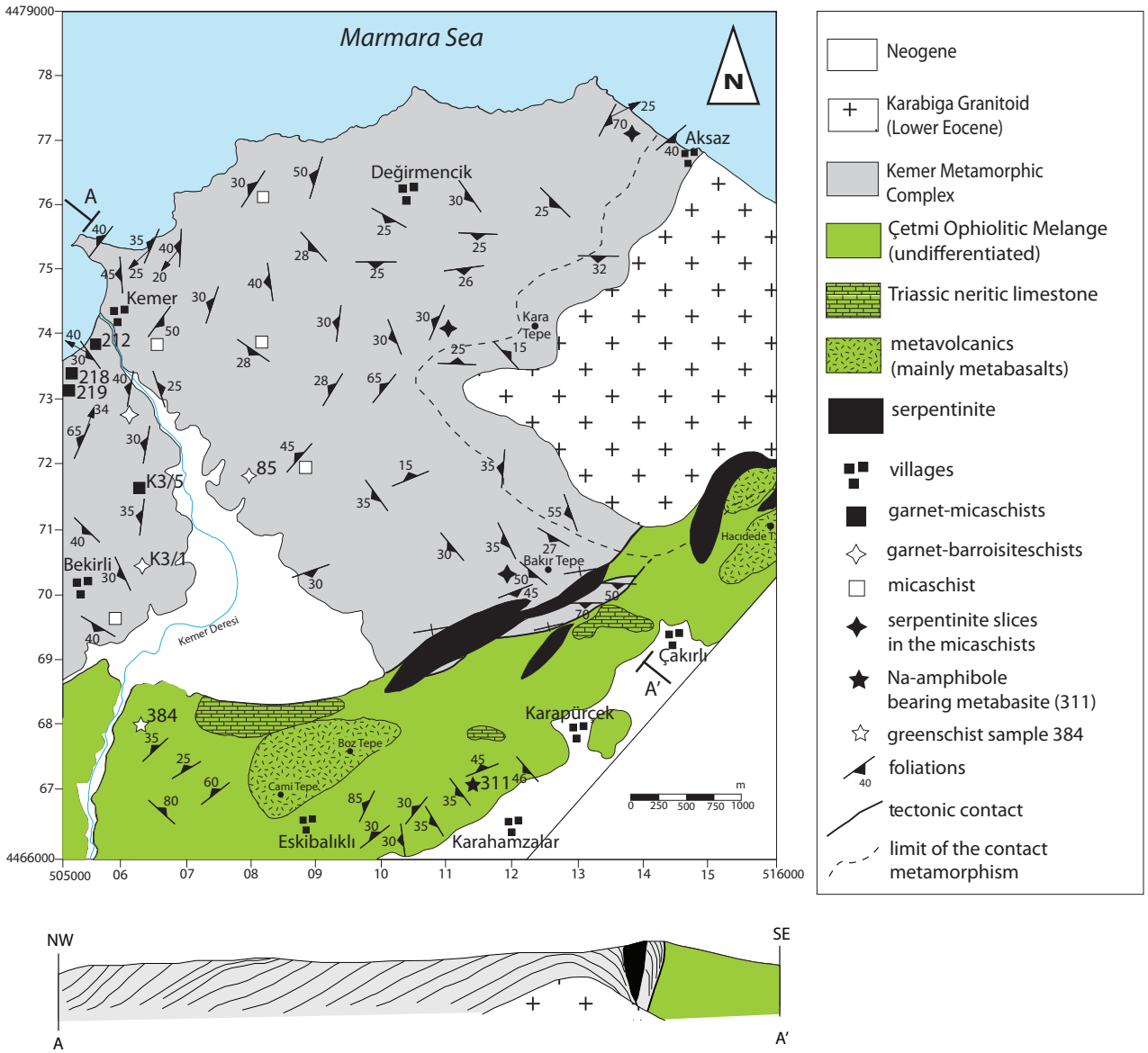

Figure 3. Geological map of the study area. For the location see Figure 2.

The metabasites consist of garnet, barroisite, epidote, albite, titanite, quartz, phengite and chlorite. Poikilitic garnet porphyroblasts, 1–3 mm across, with inclusions of epidote, rutile, titanite and quartz, are set in a foliated matrix of barroisite, phengite, quartz, epidote and albite. Large phengite flakes show replacement by fine-grained muscovite along their margins. Chlorite generally occurs as a secondary phase replacing garnet. Barroisite constitutes the bulk of the rock and occurs as bluish-green prismatic grains, 0.5–0.8 mm long. Two metabasite samples were analyzed by electron microprobe (Tables 1 & 2). Garnets from the metabasites have a compositional range of $Alm_{55-67}Grs_{22-29}Sps_{13-03}Pyp_{04-08}$. They generally show prograde zoning with rimward increase in X_{Alm} and X_{Pyp} and decrease in X_{Sps} (Figure 4c), although not as strong as in garnet from the metapelites. Amphiboles are barroisitic in composition with Na_B content ranging between 0.33–1.0 and increasing rimward. Actinolite replaces the barroisite. The $Fe^{3+}/(Fe^{3+}+Al)$ ratios of the epidotes range between 0.14 and 0.22 and show oscillatory

Table 1. Estimated modal amount of analysed samples.

	Garnet-mica schists					Garnet-amphiboleschists	
	212	218	219	226A	K3/5	85*	K3/1
Garnet	3	4	4	5	8	7	2
White mica	34_{phe}	26_{phe}	35_{phe}	40_{phe}	$40_{phe,pa}$	8_{phe}	–
Secondary muscovite	–	3	2	–	–	–	–
Albite	10	15	10	15	10	6	15
Quartz	35	34	35	25	34	20	12
Epidote	4	3	3	5	2	10	4
Chlorite	8	11	6	4	4	-	11
Calcite	6	4	5	4	-	-	-
Titanite	tr	–	tr	2	2	tr	tr
Ilmenite	–	tr	tr	–	–	–	–
Turmaline	tr	tr	tr	tr	tr	–	–
Apatite	tr	–	–	–	tr	–	tr
Na-Ca-amphibole	–	–	–	–	–	35	56
Na-amphibole	–	–	Inc.	–	–	–	–
Chloritoid	Inc.	–	–	–	–	–	–

phe, phengite; pa, paragonite; inc, inclusion; tr < 0,5

zoning. The white micas are phengitic with Si p.f.u. of 3.31 to 3.45. Plagioclases are albite. Titanite occurs both as a matrix phase and as inclusions in garnet. Rutile is only found as inclusions in garnet: some of it is replaced by titanite.

Metamorphic Conditions

The peak temperature of metamorphism is estimated from the Fe-Mg partitioning between the garnet and phengite. The Green & Hellman (1982) experimental calibration gives a temperature of 560–620°C for a given pressure of 10 kbar, whereas the Model B of Wu *et al.* (2002) indicates temperatures of 560–640°C for the same pressure. The mineral assemblages are not suitable for tightly constraining metamorphic pressures. In the absence of the limiting assemblage, the Si content of phengite gives only a minimum pressure of 10 kbar (Massonne & Schreyer 1987); maximum pressures are provided by the upper baric limit of paragonite (Figure 6). Na-amphibole and chloritoid are found as inclusions in the garnets. The reactions, which cause the consumption of the chloritoid and Na-amphibole are shown in Figure 8. They are calculated by the THERMOCALC (v. 3.25) program of Powell & Holland (1988), which use the internally consistent thermodynamic data set of Holland & Powell (1998). We used the AX program (http://rock.esc.cam.ac.uk/astaff/holland/ax.html) to calculate activities from mineral compositions.

Age of Metamorphism

The oldest lithology that unconformably overlies the metamorphic rocks is Priabonian reef limestone interbedded with volcanic tuff and conglomerate (Sirel & Acar 1982; Ercan Özcan, personal communication). Furthermore, the Kemer Metamorphic Complex and the Çetmi Mélange are intruded by an Early Eocene (52 Ma, Bacceletto *et al.* 2007) granitoid, which provides a lower age limit for the metamorphism and indicates that the metamorphic rocks were

Table 2. Representative mineral compositions of the samples 212, 219, 85 and 311.

	212					219					85					311				
	grt	phe	ep	chl	ctd (inc)	grt	phe	ep	chl	gln (inc)	grt (core)	grt (rim)	bar	phe	ep	gln	law	phe	cpx	na-ca amp
SiO_2	37.04	51.48	38.29	27.15	23.76	37.43	52.39	38.23	23.93	57.22	37.23	37.77	48.27	50.78	38.12	56.57	39.96	54.29	50.94	51.88
TiO_2	0.40	0.17	0.15	bdl	0.06	0.16	0.20	0.14	0.08	0.04	0.08	0.08	0.25	0.31	0.08	0.04	0.08	0.03	0.69	1.02
Al_2O_3	21.02	28.27	27.40	19.40	40.31	21.10	29.23	27.32	21.84	11.58	21.09	21.78	12.23	27.89	27.91	8.09	32.22	26.02	5.05	1.72
Cr_2O_3	0.03	0.02	0.01	0.03	0.02	bdl	0.14	0.17	0.07	0.05	bdl	0.11	0.04	0.02	0.08	0.02	0.01	bdl	bdl	0.01
FeO	30.54	2.66	7.96	25.64	25.12	29.15	3.26	7.85	27.80	16.22	30.38	28.23	13.64	3.04	6.65	18.02	0.83	3.61	18.66	20.16
MnO	0.50	0.07	0.16	0.59	0.11	0.42	0.04	0.55	0.25	0.06	1.38	1.23	0.22	bdl	0.05	0.13	bdl	0.04	0.21	0.36
MgO	0.97	2.65	0.01	12.01	2.01	0.92	2.83	bdl	12.25	6.08	1.82	2.28	11.01	3.15	0.03	7.03	0.11	3.76	5.58	11.54
CaO	9.57	bdl	23.47	0.54	0.09	10.80	bdl	22.93	0.04	0.27	8.00	9.46	7.48	0.06	23.24	0.41	16.56	0.31	8.45	6.10
Na_2O	0.04	0.34	0.02	0.03	bdl	bdl	0.28	bdl	bdl	5.93	0.02	0.02	3.47	0.36	bdl	6.94	0.02	0.21	7.76	4.70
K_2O	bdl	9.83	bdl	0.25	bdl	0.03	9.78	bdl	0.08	0.01	0.02	0.01	0.30	9.82	0.01	0.01	0.09	8.13	0.05	0.87
Total	100.10	95.48	97.48	85.64	91.48	100.01	98.14	97.18	86.33	97.46	100.00	100.96	96.91	95.43	96.16	97.24	89.87	96.39	97.39	98.36
Oxygen	*12*	*11*	*12.5*	*14*	*12*	*12*	*11*	*12.5*	*14*	*23*	*12*	*12*	*23*	*11*	*12.5*	*23*	*8*	*11*	*6*	*23*
Si	2.972	3.410	3.000	2.941	1.993	2.992	3.382	2.986	2.607	8.037	2.983	2.972	6.853	3.380	2.995	8.028	2.053	3.534	1.928	7.432
Ti	0.024	0.008	0.009	0.000	0.004	0.010	0.010	0.008	0.007	0.004	0.005	0.005	0.027	0.016	0.004	0.004	0.003	0.001	0.020	0.110
Al	1.988	2.207	2.530	2.477	3.985	1.988	2.224	2.515	2.804	1.917	1.992	2.020	2.046	2.188	2.584	1.354	1.951	1.996	0.225	0.290
Cr	0.002	0.001	0.000	0.002	0.001	0.000	0.007	0.010	0.006	0.005	0.000	0.007	0.004	0.001	0.005	0.003	0.000	0.000	0.000	0.001
Fe^{2+}	2.049	0.147	0.000	2.323	1.762	1.949	0.176	0.000	2.533	1.905	2.036	1.858	0.528	0.169	0.000	1.652	0.036	0.196	0.140	0.642
Fe^{3+}	0.000	0.000	0.469	0.000	0.000	0.000	0.000	0.512	0.000	0.000	0.000	0.000	1.091	0.000	0.437	0.486	0.000	0.000	0.451	1.773
Mn	0.034	0.004	0.011	0.054	0.008	0.029	0.002	0.036	0.023	0.007	0.093	0.082	0.026	0.000	0.004	0.016	0.000	0.002	0.007	0.044
Mg	0.116	0.262	0.001	1.939	0.251	0.110	0.272	0.000	1.989	1.273	0.217	0.267	2.331	0.313	0.003	1.487	0.008	0.365	0.315	2.465
Ca	0.823	0.000	1.970	0.063	0.008	0.925	0.000	1.919	0.004	0.041	0.687	0.798	1.138	0.004	1.956	0.062	0.912	0.021	0.343	0.937
Na	0.007	0.044	0.003	0.006	0.000	0.000	0.035	0.000	0.001	1.616	0.003	0.003	0.956	0.047	0.000	1.908	0.002	0.027	0.570	1.306
K	0.000	0.830	0.000	0.034	0.000	0.003	0.805	0.000	0.011	0.002	0.002	0.001	0.055	0.833	0.001	0.001	0.006	0.675	0.002	0.158
Total	8.013	6.914	7.994	9.840	8.011	8.005	6.913	7.987	9.986	14.807	8.018	8.012	15.055	6.950	7.989	15.001	4.972	6.818	4.000	15.158

bdl– below detection limit.

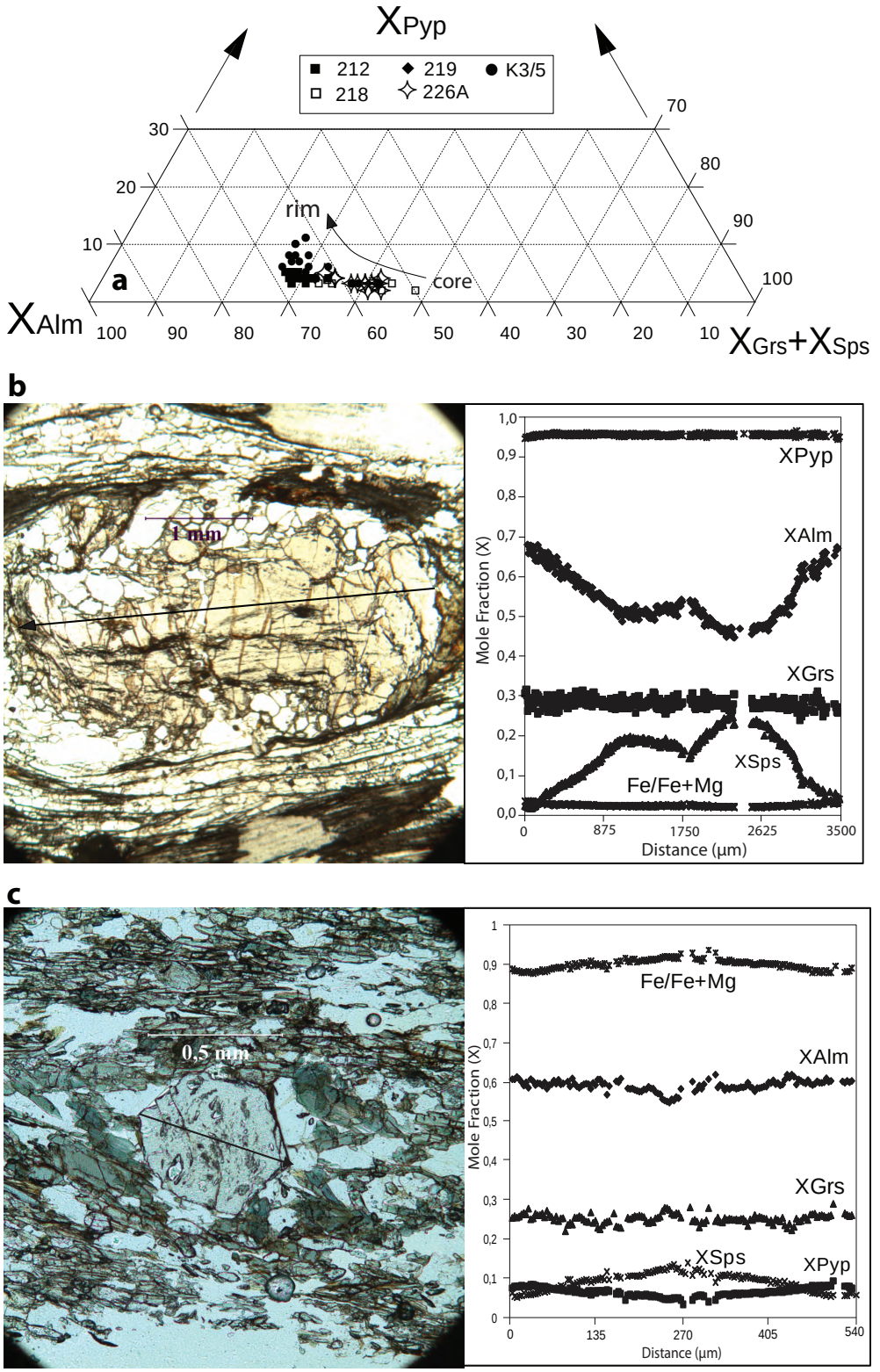

Figure 4. **(a)** Compositional variation of garnet from the mica schists. **(b)** Garnet zoning profile from sample 218 (garnet-micaschist) and photomicrograph, indicating the position of the profile parallel to the foliation. There is syn-growth of two garnet nuclei, which can be distinguished close to 1750 μm. **(c)** Garnet zoning profile from sample K3/1 (garnet-barroisiteschist).

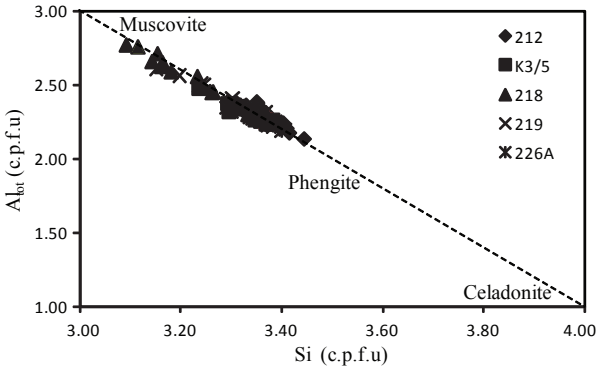

Figure 5. Composition range of white mica in the garnet-mica schists.

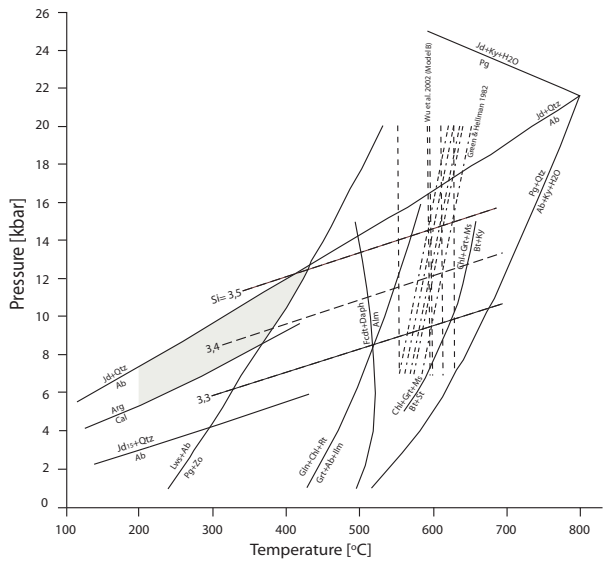

Figure 6. Estimated P-T conditions for the Kemer Metamorphic Complex and Na-amphibole-lawsonite bearing metabasite (sample 311) from the Çetmi Mélange (shaded area).

already at a high crustal level in the Early Eocene. To further constrain the age of regional metamorphism, phengitic micas from four garnet-mica schists were dated by the Rb-Sr phengite-whole rock method. The analytical procedures are given in the Appendix. The dated samples were the same as those analysed by the electron microprobe and predominantly consist of phengite, quartz and albite (Tables 1 & 2). The Rb-Sr phengite ages are 84.3±1.3 Ma, 77.7±1.9 Ma, 76±2 Ma and 63.9±1.5 Ma (Table 3). The age values show a wide scatter but indicate cooling in the Late Cretaceous below 500°C, the approximate closure temperature of muscovite for the Rb-Sr system (e.g., Cliff 1985; Villa 1998). These ages are in accordance with previously reported Late Cretaceous Rb-Sr phengite ages (69 Ma, 69±2 Ma and 65±0.9 Ma) from the Çamlıca Metamorphic Complex (Figure 2) from the central part of the Biga Peninsula (Okay & Satır 2000a) and underscore the wide extent of Late Cretaceous metamorphism in the northern Aegean.

Çetmi Mélange

The Çetmi Mélange consists of basalt, metabasite, limestone, greywacke, shale, serpentinite and radiolarian chert, occurring as tectonic slices and blocks in a poorly defined sheared slaty matrix. Spilitised basalts are the most common lithology; they generally preserve their igneous texture but show growth of new minerals including actinolite and chlorite. More importantly some of the basalts show growth of the high pressure minerals sodic amphibole, lawsonite and sodic pyroxene. The limestones in the mélange are of two types: the first type is white, thickly bedded to massive neritic limestone, yielding Late Triassic stratigraphic ages (Okay *et al.* 1991; Beccaletto *et al.* 2005). The second type is thinly bedded, pelagic limestone, often intercalated with radiolarian chert. Okay *et al.* (1991) described a composite tectonic block from the Çetmi Mélange north of Karapürçek, where the shallow marine Upper Triassic (Norian) limestone is unconformably overlain by Cretaceous (Cenomanian–Turonian) pelagic limestone and shale. Beccaletto *et al.* (2005) also describe a block with Upper Triassic neritic limestone overlain by latest Albian to Cenomanian tuff, carbonate-rich sandstone and microconglomerate. Radiolaria from the chert blocks have ages ranging from Mid Jurassic to Early Cretaceous (Beccaletto *et al.* 2005). The youngest age from the radiolarian cherts is Hauterivian–Aptian. Palynomorphs from the shales yielded Early to Middle Albian ages (Beccaletto *et al.* 2005). In conclusion the Çetmi Mélange comprises Triassic to Cretaceous sedimentary rocks; the youngest blocks are Cenomanian–Turonian in the north and Turonian–Santonian in the south around Küçükkuyu (Brinkmann *et al.* 1977; Okay *et al.* 1991).

The discovery of high-pressure minerals in one foliated metabasalt in the Çetmi Mélange is important. The sample (311) consists of sodic

Table 3. Phengite-whole rock Rb-Sr isotope analyses and the calculated age values.

	Rb [ppm]	Sr [ppm]	$^{87}Rb/^{86}Sr$	$^{87}Sr/^{86}Sr$ (2σ)	Initial $^{87}Sr/^{86}Sr$ (2σ)	Age [Ma, 2σ]
212 WR	113.6	258.5	1.2722	0.711251 (10)	0.70973 (22)	84.3±1.3
212 Phe	409.2	52.29	22.710	0.736929 (10)		
218 WR	109,8	116.6	2.7258	0.713883 (09)	0.71141 (25)	63.9±1.5
218 Phe	399.5	60.72	19.077	0.728719 (07)		
219 WR	126.5	100.5	3.6411	0.714024 (09)	0.71007 (29)	76.0±2.0
219 Phe	334.4	60.67	15.979	0.727417 (10)		
226A WR	99.80	440.4	0.6557	0.708826 (08)	0.70810 (22)	77.7±1.9
226A Phe	322.2	72.81	12.822	0.722257 (10)		

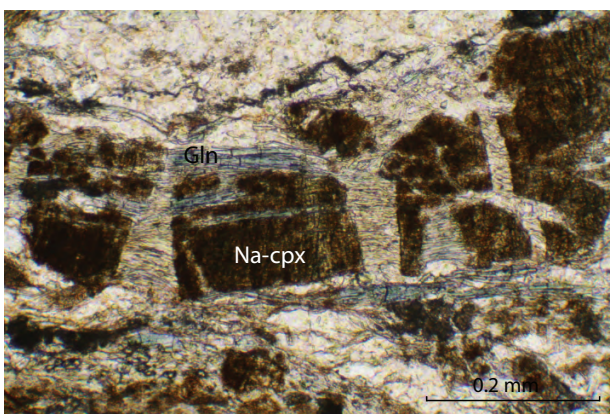

Figure 7. Boudinaged sodic pyroxene grains partly replaced by blue sodic amphibole (sample 311; photomicrograph plain polarized light).

pyroxene pseudomorphs after augite surrounded by a mylonitic foliation defined by parallel-aligned chlorite, sodic and sodic-calcic amphibole, albite, quartz, aragonite, titanite and phengite (Figure 7). Sodic amphibole occurs both as fibrous crystals defining the foliation and as small prismatic grains. It replaces an earlier green sodic-calcic amphibole. Augite is completely pseudomorphed by brownish red sodic pyroxene. Sodic pyroxene also occurs as radiating acicular rosettes associated with albite and quartz. Aragonite with characteristic lamellar twinning forms large grains, up to 2 mm across. Lawsonite has Fe_2O_3 contents between 1.82 and 2.33 wt%. The Na_B content of the Na-amphiboles (ferroglaucophane and crossite) ranges between 1.60 and 1.92 and increases rimwards (Figure 8). Metamorphic Na-Ca amphiboles are rich in alkali elements with Na_B content ranging between 0.81–1.38 and Na_A between 0.26–0.97, indicating a richterite-magnesiokatophorite composition. Na-clinopyroxenes are aegerine with 7 to 17 mol% jadeite content. White micas are phengitic with Si 3.5–3.6 p.f.u.

The other analyzed metabasite sample (384) is a typical greenschist consisting of actinolite, albite, chlorite and epidote with minor leucoxene and phengite. The tschermakite component of the actinolite decreases rimwards. The $Fe^{3+}/(Fe^{3+}+Al)$ ratios of the epidotes range between 0.18–0.30 and exhibit oscillatory zoning. The Si content in the phengites ranges between 3.30–3.36 per formula unit.

P-T Conditions in the Çetmi Mélange

The Çetmi Mélange comprises lithologies ranging from fossiliferous, unmetamorphosed limestones to foliated metabasites with blueschist- and greenschist-facies mineral assemblages. The metamorphic blocks most probably represent subducted oceanic crust, which were tectonically emplaced in the trench sediments. The P-T conditions of the metabasites

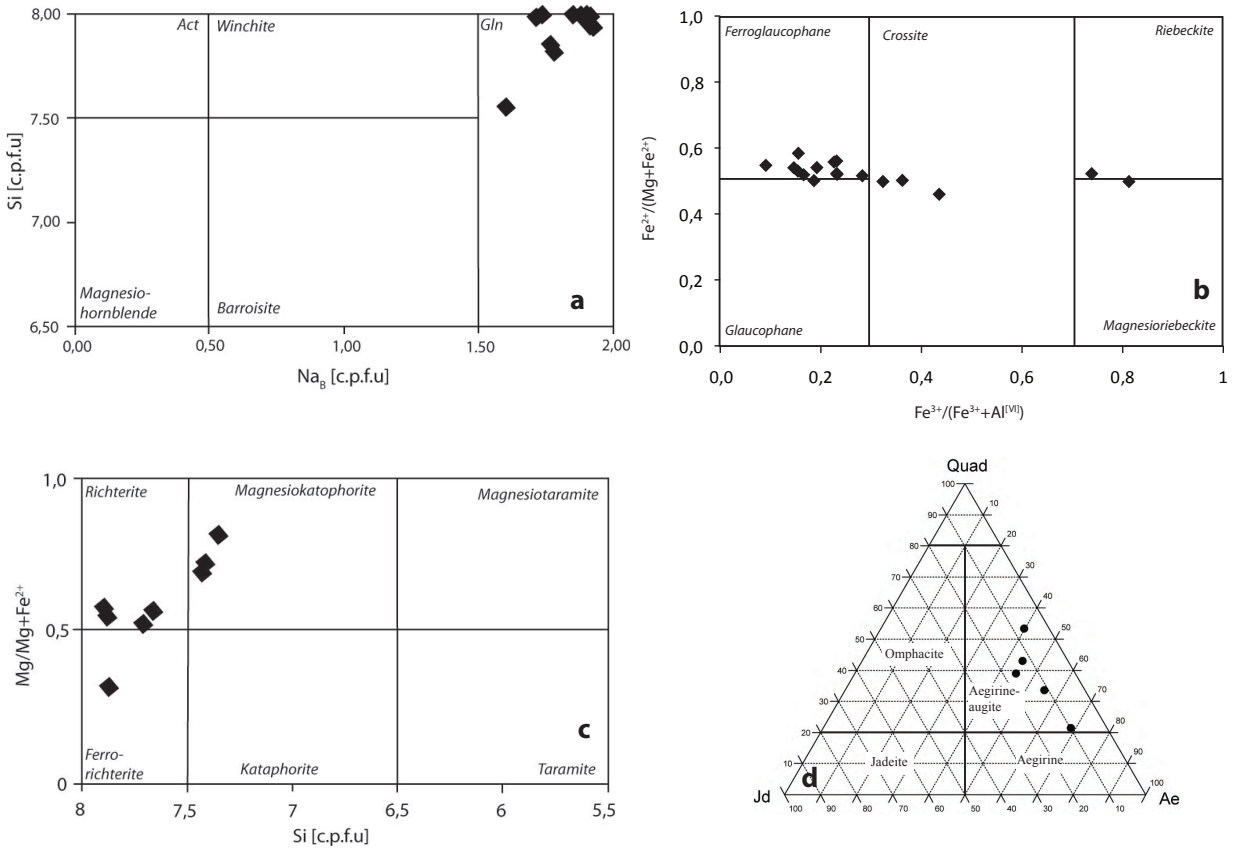

Figure 8. Compositions of the Na-amphibole **(a, b)**, Na-Ca-amphibole **(c)** and Na-clinopyroxene **(d)** in the metabasite (sample 311).

indicate the depth of subducted oceanic crust during the generation of the Çetmi Mélange. The estimation of the P-T conditions in these very low-grade metamorphic rocks is difficult due to incomplete equilibration caused by slow reaction rates at low temperatures, and the lack of reliable activity-composition data for the low-temperature minerals (Schiffman & Day 1999; Spaggiari *et al.* 2002). For the blueschist sample 311, the presence of albite gives an upper pressure limit of 8.6 kbar for an assumed temperature of 250°C (Figure 6). A lower pressure limit of 3.7 kbar is given by the jadeite content (Jd_{15}) of the sodic pyroxene for the same temperature. Aragonite gives a minimum pressure of 6±1 kbar for the 200–300°C temperature range. The occurrence of lawsonite and albite, and absence of epidote and paragonite indicate that the rock did not exceed the reaction Lws + Ab = Pg + Zo which limits the temperature below 325±35°C (Figure 6).

Discussion

High-pressure metamorphic rocks of continental affinity and oceanic accretionary complexes crop out widely throughout the Biga and Gelibolu peninsulas and indicate the consumption of a former oceanic domain followed by continental subduction. The new petrological and geochronological data and the available biostratigraphic data place constraints on the evolution of the region. The presence of blueschists in the Çetmi Mélange clearly indicate its subduction-accretion origin; the biostratigraphic data from the mélange suggest the subduction of oceanic crust and a passive continental margin of Triassic to Late Cretaceous (Turonian–Santonian) age. The tectonic setting of the Çetmi Mélange indicates that this ocean was situated between the Sakarya Zone and the Rhodope-Strandja Massif. The age span of high-pressure metamorphism in the Biga Peninsula and southern Thrace indicate the duration

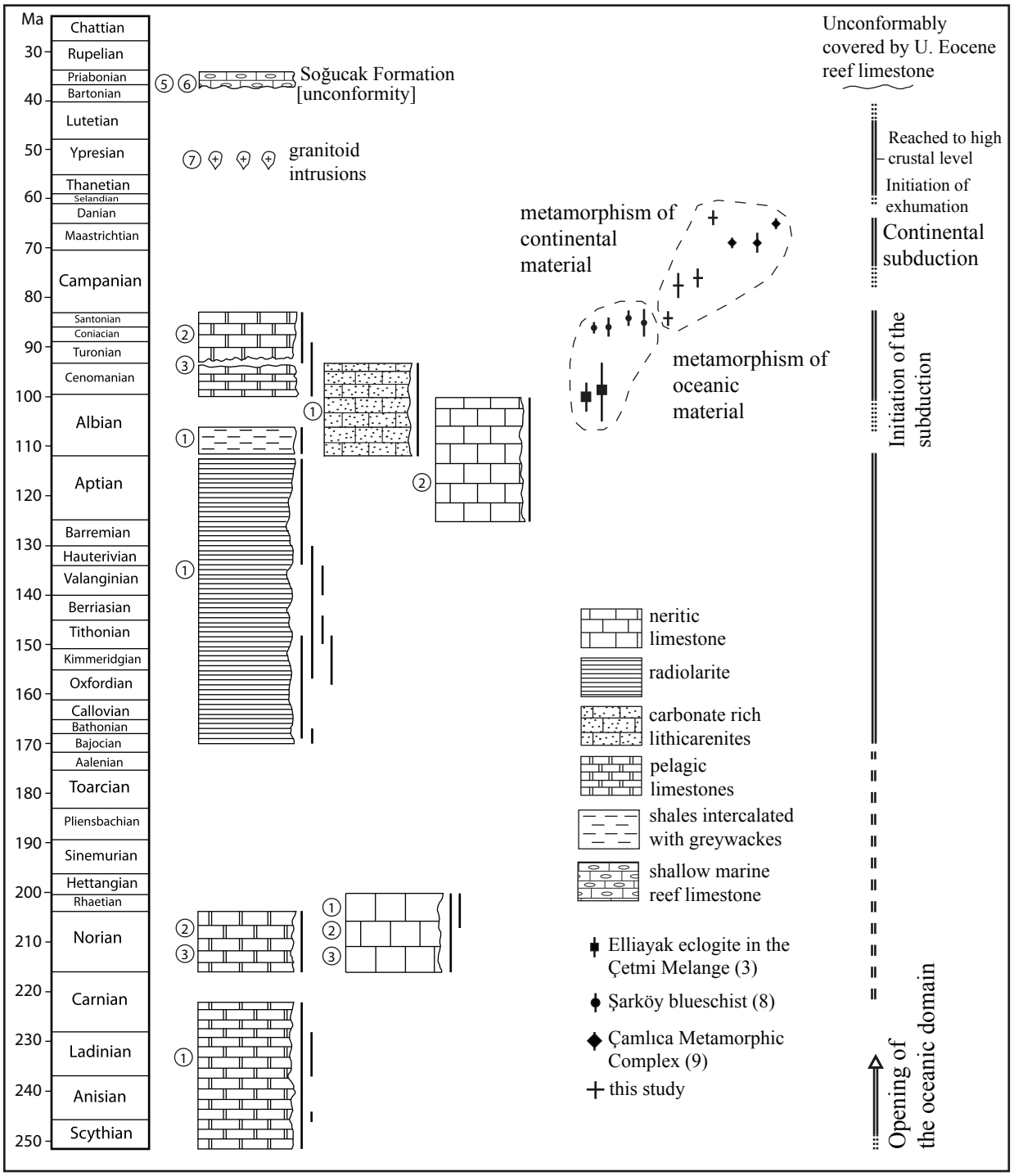

Figure 9. The age range of the tectonic blocks in the Çetmi Mélange and Çamlıca-Kemer Metamorphic Complex from this study compared to literature data for biostratigraphic and isotopic ages, and their interpretation in terms of geodynamic evolution. References: (1) Beccaletto *et al.* 2005, (2) Okay *et al.* 1991, (3) Okay & Satır 2000b, (4) Bringman *et al.* 1977, (5) Özcan *et al.* 2010, (6) Sirel & Acar 1982, (7) Beccaletto *et al.* 2007, (8) Topuz *et al.* 2008, (9) Okay & Satır 2000a.

of the subduction. The Rb-Sr ages from the eclogites in the Çetmi Mélange from its southern outcrop are *ca.* 100 Ma and indicate ongoing subduction during the Albian (Okay & Satır 2000b). Blueschists with ophiolitic protoliths from southern Thrace have given *ca.* 86 Ma Rb-Sr and Ar-Ar ages (Topuz *et al.* 2008) and indicate subduction continuing until the Coniacian–Campanian (Figure 9). Our Rb-Sr ages from the Kemer Metamorphic Complex, as well as those from the Çamlıca Metamorphic Complex (Okay & Satır 2000a) range between 84 and 65 Ma. Although there is a wide scatter, the ages are younger than those from the high-pressure metamorphic rocks with oceanic affinity. It is likely that the Kemer-Çamlıca Metamorphic Complex represents a continental margin or a small continental block, which was pulled into the subduction zone following the complete consumption of the oceanic lithosphere. Finally, the Kemer Metamorphic Complex started to exhume in the Palaeocene, as reflected by extension-related ductile to brittle-ductile shearing (Beccaletto *et al.* 2007).

Summary

The northern Biga Peninsula exposes high-pressure rocks of continental affinity, the so-called Kemer Metamorphic Complex, which are in tectonic contact with an oceanic accretionary complex. This metamorphic complex is comparable with the Çamlıca Metamorphic Complex further west. Over 90% of the Kemer Metamorphic Complex is composed of metapelitic mica schist, calcschist and marble, which indicate a continental margin rather than oceanic accretionary setting for the protolith. Northward subduction under the Strandja-Rhodope Zone is indicated by the Upper Cretaceous magmatic rocks in the Sredna-Gora and in the northern parts of the Rhodope-Strandja Zone. Therefore, the Kemer Metamorphic Complex represents the northern continental margin of the Sakarya Zone. A separate origin as a small continental block for the high-pressure rocks is also possible, although this would require a distinct suture zone straddling the small continental block and Sakarya Zone, and this is unknown so far. Moreover, biostratigraphic and geochronological data suggest a single continuous and concordant Albian to latest Maastrichtian subduction-accretion process for the Biga Peninsula. Consequently, the Late Cretaceous convergence led to frontal accretionary continental growth of the Rhodope-Strandja Zone and final continental subduction of the continental margin of the Sakarya Zone. The convergence is constrained to the Late Cretaceous–Early Eocene interval by the Early Eocene (52 Ma) Karabiga granitoid, which intrudes both the Çetmi Mélange and Kemer Metamorphic Complex.

Acknowledgements

This study presents the main results of a MSc Thesis. We thank Gisela Bartholomä for help in the mineral separation, Mehmet Ali Oral for the preparation of thin sections and Elmar Reitter for the isotopic measurements. We also thank an anonymous reviewer for constructive comments.

References

Beccaletto, L. & Jenny, C. 2004. Geology and correlation of the Ezine Zone: a Rhodope fragment in NW Turkey? *Turkish Journal of Earth Sciences* **13**, 145–176.

Beccaletto, L., Bartolini, A.C., Martini, R., Hochuli, P.A. & Kozur, H. 2005. Biostratigraphic data from Çetmi Melange, northwest Turkey: palaeogeographic and tectonic implications. *Palaeogeography, Palaeoclimatology, Palaeoecology* **221**, 215–244.

Beccaletto, L., Bonev, N., Bosch, D. & Bruguier, O. 2007. Record of a Palaegene syn-collisional extension in the north Aegean region: evidence from the Kemer micaschists (NW Turkey). *Geological Magazine* **144**, 393–400.

Bonev, N. & Stampfli, G. 2008. Petrology, geochemistry and geodynamic implications of Jurassic island arc magmatism as revealed by mafic volcanic rocks in the Mesozoic low-grade sequence, eastern Rhodope, Bulgaria. *Lithos* **100**, 210–233.

Brinkmann, R., Gümüş, H., Plumhoff, F. & Salah, A.A. 1977. Höhere Oberfreide in nordwest Anatolien und Thrakien. *Neues Jahrbuch für Geologie und Paleontologie Abhandlungen* **154**, 1–20.

Burg, J.P., Ricou, L.E., Ivanov, Z., Godfriaux, I., Dimov, D. & Klain, L. 1996. Syn-metamorphic nappe complex in the Rhodope Massif: structure and kinematics. *Terra Nova* **8**, 6–15.

Cliff, R.A. 1985. Isotopic dating in metamorphic belts. *Journal of the Geological Society, London* **142**, 97–110.

Green, T.H. & Hellman, P.L. 1982. Fe-Mg partitioning between coexisting garnet and phengite at high pressure, and comments on a garnet-phengite geothermometer. *Lithos* **15**, 253–266.

Holland, T. & Powell, R. 1998. An internally consistent thermodynamic data set for phases of petrological interest. *Journal of Metamorphic Geology* **16**, 309–343.

Konak, N. 2002. *Geological Map of Turkey. İzmir Sheet, Scale 1:500.000*. Publication of the General Directorate of the Mineral Research and Exploration (MTA), Ankara.

Magganas, C.A. 2002. Constraints on the petrogenesis of Evros ophiolite extrusives, NE Greece. *Lithos* **65**, 165–182.

Massonne, H.J. & Schreyer, W. 1987. Phengite geobarometry based on the limiting assemblage with K-feldspar, phlogopite and quartz. *Contribution to Mineralogy and Petrology* **96**, 212–224.

Mposkos, E. & Kostopoulos, D. 2001. Diamond, former coesite and supersilicic garnet in metasedimentary rocks from the Greek Rhodope: a new ultrahigh-pressure metamorphic province established. *Earth and Planetary Science Letters* **192**, 497–506.

Okay, A.I. 1989. Tectonic units and sutures in the Pontides, Northern Turkey. *In*: Şengör, A.M.C. (ed), *Tectonic Evolution of the Tethyan Region*. Kluwer Academic Publishers, 109–116.

Okay, A.I. & Göncüoğlu, M.C. 2004. Karakaya Complex: a review of data and concepts. *Turkish Journal of Earth Sciences* **13**, 77–95.

Okay, A.I. & Monie, P. 1997. Early Mesozoic subduction in the Eastern Mediterranean: evidence from Triassic eclogite in northwest Turkey. *Geology* **25**, 595–598.

Okay, A.I., Monod, O. & Monie, P. 2002. Triassic blueschists and eclogites from northwest Turkey: vestiges of the Paleo-Tethyan subduction. *Lithos* **64**, 155–178.

Okay, A.I. & Satir, M. 2000a. Upper Cretaceous eclogite-facies metamorphic rocks from the Biga Peninsula, Northwest Turkey. *Turkish Journal of Earth Sciences* **9**, 47–56.

Okay, A.I. & Satir, M. 2000b. Coeval plutonism and metamorphism in a latest Oligocene metamorphic core complex in northwest Turkey. *Geological Magazine* **137**, 495–516.

Okay, A.I., Siyako, M. & Bürkan, K.A. 1991. Geology and tectonic evolution of the Biga Peninsula, northwest Turkey. *Bulletin of the İstanbul Technical University* **44**, 191–256.

Okay, A.I., Satir, M., Maluski, H., Siyako, M., Monie, P., Metzger, R. & Akyüz, S. 1996. Palaeo- and Neo-Tethyan events in northwest Turkey. *In*: Yin, E. & Harrison, M. (eds), *Tectonics of Asia.* Cambridge University Press, 420–441.

Okay, A.I., Satir, M. & Siebel, W. 2006. Pre-Alpide Palaeozoic and Mesozoic orogenic events in the Eastern Mediterranean region. *In*: Gee, D.G. & Stephenson, R.A. (eds), *European Lithosphere Dynamics*. Geological Society, London, Memoirs **32**, 389–405.

Okay, A.I., Satir, M., Tüysüz, O., Akyüz, S. & Chen, F. 2001. The tectonics of the Strandja Massif: late-Variscan and mid-Mesozoic deformation and metamorphism in the northern Aegean. *International Journal of Earth Sciences* **90**, 217–233.

Okay, A.I. & Tansel, İ. 1994. New data on the upper age of the Intra-Pontide ocean from north of Sarköy (Thrace). *Bulletin of Mineral Research and Exploration* **114**, 23–26.

Okay, A.I & Tüysüz, O. 1999. Tethyan sutures of northern Turkey. *In*: Durand, B., Jolivet, L., Horvath, F. & Seranne, M. (eds), *The Mediterranean Basins: Tertiary Extension Within the Alpine Orogen*. Geological Society, London, Special Publications **156**, 475–515.

Okay, A.I., Özcan, E., Cavazza, W., Okay, N. & Less, G. 2010. Basement types, Lower Eocene series, Upper Eocene olistostromes and the initiation of the southern Thrace Basin, NW Turkey. *Turkish Journal of Earth Sciences* **19**, 1–25.

Özcan, E., Less, G., Okay, A.I., Báldi-Beke, M., Kollanyi, K. & Yilmaz, İ. Ö. 2010. Stratigraphy and larger foraminifera of the Eocene shallow-marine and olistostromal units of the southern part of the Thrace Basin, NW Turkey. *Turkish Journal of Earth Sciences* **19**, 27–77.

Pouchou, J.L. & Pichoir, F. 1984. A new model for quantitative analyses. I. Application to the analysis of homogeneous samples. *La Recherche Aerospatiale* **3**, 13–38.

Pouchou, J.L. & Pichoir, F. 1985. 'PAP' (f-r-Z) correction procedure for improved quantitative microanalysis. *In*: Armstrong, J.T (ed), *Microbeam Analysis*. San Francisco Press, San Francisco, CA, 104–106.

Powell, R. & Holland, T. 1988. An internally consistent thermodynamic dataset with uncertainties and correlations: 3. Application methods, worked examples and a computer program. *Journal of Metamorphic Geology* **6**, 173–204.

Ricou, L.E., Burg, J.P., Godfriaux, I. & Ivanov, Z. 1998. Rhodope and Vardar: the metamorphic and the olistostromic paired belts related to the Cretaceous subduction under Europe. *Geodinamica Acta* **11**, 285–309.

Schiffman, P. & Day, H.W. 1999. Petrological methods for the study of very low-grade metabasites. *In*: Frey, M. & Robinson, D. (eds), *Low-Grade Metamorphism*. Blackwell Science Ltd., Oxford, London.

Şengör, A.M.C & Yilmaz, Y. 1981. Tethyan evolution of Turkey: a plate tectonic approach. *Tectonophysics* **75**, 181–241.

Sirel, E. & Acar, Ş. 1982. Praebullalveolina, a new foraminifal genus from the Upper Eocene of the Afyon and Çanakkale region (west of Turkey). *Eclogae Geologicae Helvetiae* **75**, 821–839.

Spaggiari, C.V., Gray, D.R. & Foster, D.A. 2002. Blueschist metamorphism during accretion in the Lachlan Orogen, south-eastern Australia. *Journal of Metamorphic Geology* **20**, 711–726.

Sunal, G., Natal'in, B., Satir, M. & Toroman, E. 2006. Paleozoic magmatic events in the Strandja Massif, NW Turkey. *Geodinamica Acta* **19**, 283–300.

Sunal, G., Satir, M., Natalin, B.A., Topuz, G. & Vonderschmidt, O. 2011. Metamorphism and diachronous cooling in a contractional orogen: the Strandja Massif, NW Turkey. *Geological Magazine* **148**, 580–596.

Sunal, G., Satir, M., Natalin, B.A. & Toraman, E. 2008. Paleotectonic position of the Strandja Massif and surrounding continental blocks based on zircon Pb-Pb age studies. *International Geology Review* **60**, 519–545.

Topuz, G., Altherr, R., Kalt, A., Satir, M., Werner, O. & Schwarz, W.H. 2004a. Aluminous granulites from the Pulur complex, NE Turkey: a case of partial melting, efficient melt extraction and crystallisation. *Lithos* **72**, 183–207.

Topuz, G., Altherr, R., Satir, M. & Schwartz, W.H. 2004b. Low-grade metamorphic rocks from the Pulur Complex, NE Turkey: implications for the pre-Liassic evolution of the Eastern Pontides. *International Journal of Earth Sciences* **93**, 72–91.

Topuz, G., Altherr, R., Schwartz, W.H., Dokuz, A. & Meyer, H.P. 2007. Variscan amphibolites-facies rocks from the Kurtoğlu metamorphic complex (Gümüşhane area, Eastern Pontides, Turkey). *International Journal of Earth Sciences* **96**, 861–873.

Topuz, G., Okay, A.I., Altherr, R., Satir, M. & Schwarz, W.H. 2008. Late Cretaceous blueschist facies metamorphism in southern Thrace (Turkey) and its geodynamic implications. *Journal of Metamorphic Geology* **26**, 895–913.

Topuz, G., Altherr, R., Siebel, W., Schwarz, W.H., Zack, T., Hasözbek, A., Barth, M., Satir, M. & Şen, C. 2010. Carboniferous high-potassium I-type granitoid magmatism in the Eastern Pontides: the Gümüşhane pluton (NE Turkey). *Lithos* **116**, 92–110.

Türkecan, A. & Yurtsever, A. 2002. *Geological Map of Turkey. İstanbul Sheet, Scale 1:500.000*. Publication of the General Directorate of the Mineral Research and Exploration (MTA), Ankara.

Villa, I.M. 1998. Isotopic closure. *Terra Nova* **10**, 42–47.

Wu, C.M., Wang, X.S., Yang, C.H., Geng, Y.S., & Liu, F.L. 2002. Empirical garnet-muscovite geothermometry in metapelites. *Lithos* **62**, 1–13.

Appendix

Methods

Mineral analyses were performed with the CAMECA-SX51 electron microprobe equipped with five wavelength-dispersive spectrometers at the Mineralogical

Institute of the University of Heidelberg. Natural and synthetic silicate and oxide minerals were used for the calibration. The operating conditions were 15 kV accelerating voltage, 20 nA beam current and 10 s counting time for all elements. A beam size of ~1μm was used in all analyses. Feldspars were analysed with a 10 μm beam size. Detection limits are below 0.1 wt%. Raw data were corrected for matrix effects with the help of the PAP algorithm (Pouchou & Pichoir 1984, 1985), implemented by CAMECA.

For isotope analyses, samples were dissolved in 52% HF for four days at 140°C on a hot plate. Digested samples were dried and redissolved in 6N HCL, dried again and redissolved in 2.5N HCl. Rb, Sr and LREE were isolated on quartz columns by conventional ion exchange chromatography with a 5 ml resin bed of BioRad AG 50W-X8, 200-400 mesh. Isotope analyses were made on a Finnigan MAT-262 multicollector mass spectrometer in the Institute of Geochemistry of the University of Tübingen. Sr was loaded with a Ta-HF activator on pre-conditioned W filaments and was measured in single-filament mode. Rb was loaded on pre-conditioned Re filaments and measurements were performed in a Re double filament assembly. The $^{87}Sr/^{86}Sr$ isotope ratios were normalised to $^{86}Sr/^{88}Sr= 0.1194$. The NBS 987 Sr standard yielded a $^{87}Sr/^{86}Sr$-ratio of 0.710250±0.000009. Total procedural blanks (chemistry and loading) were <250 pg for Sr.